Fission yeast Pds5 is required for accurate chromosome segregation and for survival after DNA damage or metaphase arrest

Shao-Win Wang, Rebecca L. Read and Chris J. Norbury*

Imperial Cancer Research Fund Molecular Oncology Laboratory, University of Oxford Weatherall Institute of Molecular Medicine, John Radcliffe Hospital, Oxford OX3 9DS, UK

*Author for correspondence (e-mail: norbury@icrf.icnet.uk)

Accepted 26 October 2001
Journal of Cell Science 115, 587-598 (2002) © *The Company of Biologists Ltd*

Summary

Sister chromatid cohesion, which is established during the S phase of the eukaryotic cell cycle and persists until the onset of anaphase, is essential for the maintenance of genomic integrity. Cohesion requires the multi-protein complex cohesin, as well as a number of accessory proteins including Pds5/BIMD/Spo76. In the budding yeast *Saccharomyces cerevisiae* Pds5 is an essential protein that localises to chromosomes in a cohesin-dependent manner. Here we describe the characterisation in the fission yeast *Schizosaccharomyces pombe* of *pds5*$^{+}$, a novel, non-essential orthologue of *S. cerevisiae PDS5*. The *S. pombe* Pds5 protein was localised to punctate nuclear foci in a manner that was dependent on the Rad21 cohesin component. This, together with additional genetic evidence, points towards an involvement of *S. pombe* Pds5 in sister chromatid cohesion. *S. pombe pds5* mutants were hypersensitive to DNA damage and to mitotic metaphase delay, but this sensitivity was apparently not due to precocious loss of sister chromatid cohesion. These cells also suffered increased spontaneous chromosome loss and meiotic defects and their viability was dependent on the spindle checkpoint protein Bub1. Thus, while *S. pombe* Pds5 has an important cohesin-related role, this differs significantly from that of the equivalent budding yeast protein.

Key words: *Schizosaccharomyces pombe*, Cohesin, Mitosis, Sister chromatid cohesion

Introduction

During DNA replication in eukaryotes, the newly replicated sister chromatids become stably associated along their length. Some level of sister chromatid cohesion is maintained until the onset of mitotic anaphase, and is required for the establishment of bipolar attachments to spindle microtubules, and hence for accurate chromosome segregation. Dissolution of cohesion is thought to be fundamental to the initiation of poleward chromosome movement in anaphase. Cohesion is maintained by the conserved multi-protein complex cohesin, which contains Smc1, Smc3, Scc1/Mcd1 and Scc3 (in the protein nomenclature of the budding yeast *Saccharomyces cerevisiae*), although it is not yet clear if this complex constitutes a literal protein 'bridge' between sister chromatids (Guacci et al., 1997; Losada et al., 1998; Michaelis et al., 1997). Dissolution of cohesion in *S. cerevisiae* is brought about by the Esp1-catalysed proteolysis of Scc1 (Uhlmann et al., 2000). DNA polymerase σ/Trf4 was recently shown to be required for the establishment of cohesion during S phase in *S. cerevisiae* (Wang et al., 2000b). This novel polymerase may be recruited by a replication factor C (RFC)-like complex containing Ctf18, Ctf8 and Dcc1 to replication forks that have encountered sites of cohesion (Mayer et al., 2001). Additional factors (Eco1/Ctf7/Eso1, Scc2/Mis4 and Scc4) are required for the establishment of cohesion, but not for its maintenance (Ciosk et al., 2000; Furuya et al., 1998; Tanaka et al., 2000; Tomonaga et al., 2000; Toth et al., 1999). The cohesin-associated protein Pds5 is also required for the establishment and maintenance of cohesion in *S. cerevisiae* (Hartman et al., 2000; Panizza et al., 2000), and Pds5-like proteins appear to play related roles, both in other fungi and in metazoans (Denison et al., 1993; Holt and May, 1996; Huynh et al., 1986; Sumara et al., 2000). Detailed sequence analysis has identified tandem HEAT (huntingtin, elongation factor 3, alpha subunit of protein phosphatase 2A, Tor1) repeat units in both *S. cerevisiae* Pds5 and Scc2, suggesting that in the context of these proteins this structural element might interact with cohesin (Neuwald and Hirano, 2000; Panizza et al., 2000).

S. cerevisiae Pds5 is essential for maintaining viability during the mitotic cell cycle. Temperature sensitive *S. cerevisiae pds5* mutants were identified in a screen for selective loss of viability during a brief mitotic arrest in comparison with a G1 arrest (Hartman et al., 2000). On shifting such *pds5* mutants to the restrictive temperature, most cells fail to complete mitosis, being delayed in anaphase or telophase. This terminal phenotype suggests that the cohesion-promoting activity of Pds5 is essential for cell viability. This interpretation is strengthened by the finding that the *bimD6* mutation in *A. nidulans* can be suppressed by mutation of *sudA*, which encodes an Smc3-like protein (Holt and May, 1996). The *bimD6* terminal phenotype also indicates an essential role for BIMD in the successful completion of mitosis (Denison et al., 1993). However, the *bimD6* allele contains a nonsense mutation that would be predicted to lead to the production of a short truncated peptide (van Heemst et al., 2001). Thus, the BIMD protein may be non-essential for mitotic growth at low temperatures. Spo76,

the BIMD functional homologue in *Sordaria macrospora* (van Heemst et al., 1999), is dispensable for vegetative growth, in contrast to the essential nature of *S. cerevisiae* Pds5. Although *spo76* mutants exhibit clear defects in meiotic and mitotic chromosome cohesion, in the mitotic cycle they show only a comparatively subtle delay in the transition from prometaphase to metaphase (van Heemst et al., 1999).

A. nidulans bimD mutants are hypersensitive to DNA damage (Denison et al., 1993), and this sensitivity could be attributable to a role of BIMD in chromatid cohesion. Furthermore, mutation of *Schizosaccharomyces pombe rad21* (the *SCC1* orthologue) confers defects in the repair of double-strand DNA breaks and *mis4* mutants (which are defective in cohesin loading) are sensitive to ultraviolet (UV) irradiation (Birkenbihl and Subramani, 1992; Furuya et al., 1998). Similarly, a requirement for cohesion in postreplicative DNA repair has recently been demonstrated in *S. cerevisiae* (Sjögren and Nasmyth, 2001). Cohesion therefore appears to promote DNA repair from the undamaged sister chromatid and hence affords resistance to a variety of forms of DNA damage. This interpretation is supported by the observation that, during the selection of templates for recombinational DNA repair in vivo, sister chromatids are preferred to homologous chromosomes (Kadyk and Hartwell, 1992).

Despite these studies on Pds5 and its orthologues in diverse species, there is no clear consensus regarding the role played by this protein in sister chromatid cohesion. The recent completion of the genome sequence of *S. pombe*, which is only distantly related to *S. cerevisiae*, *A. nidulans* and *S. macrospora* has allowed the identification of the only *S. pombe* gene significantly related to *PDS5*. Here, we describe the functional characterisation of this fission yeast gene, which we designate *pds5*$^+$, and its involvement in the maintenance of genome stability.

Materials and Methods

Database searches

Searches to identify Pds5-related sequences in *S. pombe* were performed using the Sanger Centre BLAST server (http://www.sanger.ac.uk/Projects/S_pombe/blast_server.shtml). Ψ-BLAST (http://www.ncbi.nlm.nih.gov/cgi-bin/BLAST/nph-psi_blast) searches were used to identify similarities between Pds5 and proteins in the Swissprot database. Megalign (DNASTAR Inc., Madison, WI) was used to generate multiple protein sequence alignments, and the sequence relatedness data shown in Fig. 1A were derived using BLAST2 (BLASTP 2.1.2; http://www.ncbi.nlm.nih.gov/gorf/bl2.html) with the values BLOSUM 62, GAP OPEN 11 and GAP EXTENSION 1. Protein sequence motifs were identified using ProfileScan (http://hits.isb-sib.ch/cgi-bin/hits_motifscan).

Fission yeast strains and methods

Conditions for growth, maintenance and genetic manipulation of fission yeast were as described previously (Moreno et al., 1991). A complete list of the strains used in this study is given in Table 1. Except where otherwise stated, strains were grown at 30°C in YE or EMM2 medium with appropriate supplements. Where necessary, gene expression from the *nmt1* promoter was repressed by the addition of 5 μM thiamine to the growth medium.

Minichromosome loss assays were performed using strains as shown in Table 1 containing the non-essential *ade6-M216* marked Ch16 minichromosome derivative of chromosome 3 (Niwa et al., 1986). The *ade6-M216* allele complements an unlinked *ade6-M210* marker in these strains such that they remain ade$^+$ as long as the minichromosome is maintained. Chromosome loss was measured in the progeny from a single ade$^+$ cell after a known number of generations during which selection for adenine prototrophy had been relaxed by growth on YE agar. Rates of chromosome loss per generation were calculated exactly as described elsewhere (Murakami et al., 1995; Stewart et al., 1997), according to the formula:

$$\text{Rate} = 1 - e^{(1/n)\ln R_n},$$

Table 1. *S. pombe* strains used in this study

Strain	Genotype	Source
HM123	*h⁻ leu1-32*	Laboratory stock
428h	*h⁻ ade6-M210 leu1-32 ura4-D18*	Laboratory stock
429h	*h⁺ ade6-M216 leu1-32 ura4-D18*	Laboratory stock
rad3Δ	*h⁻ rad3::ura4⁺ ade6-704 leu1-32 ura4-D18*	A. M. Carr
pds5Δ	*h⁺ pds5::ura4⁺ ade6-M210 leu1-32 ura4-D18*	This study
	h⁻ pds5::ura4⁺ ade6-M216 leu1-32 ura4-D18	This study
pds5Δ (*LEU2*)	*h⁻ pds5::LEU2 ade6-M216 leu1-32 ura4-D18*	This study
HM248	*h⁻ his2 ade6-M210 (Ch16 ade6-M216*)	T. Toda
pds5Δ Ch16	*h⁻ pds5::ura4⁺ ade6-M210 ura4-D18 (Ch16 ade6-M216*)	This study
pds5-GFP	*h⁻ pds5-GFP:kanMX6 leu1-32 ura4-D18*	This study
pds5-HA	*h⁻ pds5-HA:kanMX6 leu1-32 ura4-D18*	This study
nda3-KM311	*h⁺ nda3-KM311 leu1-32 ura4-D18 his2*	T. Toda
nda3-KM311 pds5Δ	*h⁺ nda3-KM311 pds5::ura4⁺ leu1-32 ura4-D18*	This study
ndc80-GFP	*h⁻ ndc80-GFP:kanMX6 leu1-32 ura4-D18*	J. V. Kilmartin
nda3-KM311 ndc80-GFP pds5Δ	*h⁺ nda3-KM311 pds5::ura4 ndc80-GFP:kanMX6 leu1-32 ura4-D18*	This study
rad21-K1	*h⁻ rad21-K1:ura4⁺ ade6-M216 leu1-32 ura4-D18 his7-366*	H. Ikeda
rad21-K1 pds5-GFP	*h⁻ rad21-K1:ura4⁺ pds5-GFP:kanMX6 ade6-M216 leu1-32 ura4-D18 his7-366*	This study
rad21-HA	*h⁻ rad21-HA:LEU2 leu1-32*	M. Yanagida
rad21-GFP	*h⁻ rad21-GFP:LEU2 leu1-32*	M. Yanagida
pds5Δ rad21-GFP	*h⁻ rad21-GFP:LEU2 pds5::ura4⁺ leu1-32 ura4-D18*	This study
rad21-K1 pds5Δ	*h⁺ h⁻ rad21-K1:ura4/rad21⁺ pds5::LEU2/pds5⁺ ade6-M210/ade6-M216 leu1-32/leu1-32 ura4-D18/ura4-D18*	This study
mis4-242	*h⁻ mis4-242 leu1-32*	M. Yanagida
pds5Δ mis4-242	*h⁻ mis4-242 pds5::LEU2 leu1-32*	This study
bub1Δ	*h⁻ bub1::LEU2 ade6-M210 leu1-32 ura4-DS/E his1-102*	J.-P. Javerzat
pds5Δ bub1Δ	*h⁻ pds5::ura4⁺ bub1::LEU2 ade6-M210 leu1-32 ura4-D18/DS/E*	This study
GFP-swi6	h⁻ ars1(MluI)::pREP81Xgfpswi6-LEU2 ade6-M210 leu1-32 ura4-D18	R. Allshire
GFP-swi6 pds5Δ	*h⁻ pds5::ura4⁺ ars1(MluI)::pREP81Xgfpswi6-LEU2 ade6-M210 leu1-32 ura4-D18*	This study

Table 2. Oligonucleotides used in this study

Name	Sequence (5′-3′)
PDS5A	GCTCTTATGGATATAGAGCATTGAAAGTTTACTGCATTTGTCATTTATTTGTTAAATACCCAAGGTGAATAGTACAAAAGAAATCCCACTGGCTATATGT
PDS5B	TCATTGGTAATATTGGGTAAGTGTTCTAGTATCGGTATTTCGCATCCAAATAAGCCTTTTTTATAAATCCTCTATTTCATAATTCTAAATGCCTTCTGAC
TAGA	AAGCACCGTCTTCAAGTGAGGAGATAAGCGAAGAAGAGGAGGAAATTAGCGAAGAAGATTTTGATGAAATAGAGGATTTACGGATCCCCGGGTTAATTAA
TAGB	ATCTAATTAACATTGAAAATTCATTGGTAATATTGGGTAAGTGTTCTAGTATCGGTATTTCGCATCCAAATAAGCCTTTTGAATTCGAGCTCGTTTAAAC

where R_n is the proportion of ade$^+$ cells *n* generations after removal of selection. For each strain tested, mean rates were calculated from five independent measurements.

Gene disruption and related techniques

The one-step disruption method was used, following PCR-mediated generation of the entire *ura4*$^+$ gene flanked by 80 bp segments from the 5′ and 3′ regions of *pds5*$^+$, using oligonucleotides PDS5A and B (Table 2). Following transformation of a diploid strain 428h/429h, ura$^+$ progeny were screened for the desired integration pattern by diagnostic PCR reactions using primer pairs spanning the presumptive recombination sites (details of the additional primers used for this purpose are available from the authors on request). Meiosis and sporulation were induced by plating onto malt extract agar, and tetrad dissection was performed with an MSM micromanipulator (Singer Instruments, UK) as described elsewhere (Moreno et al., 1991). Construction of the chromosomally HA- and GFP-tagged *pds5* strains (*pds5-HA* and *pds5-GFP*) was accomplished by an analogous method using primers TAGA and B (Table 2). The *pds5::LEU2* allele was generated by a secondary one-step disruption of the *pds5::ura4*$^+$ allele using primers as described previously (Wang et al., 2000a).

Antibodies and immunoblotting

Immunoblotting was performed essentially as described elsewhere (Ausubel et al., 1995) using Mini-Protean electrophoresis equipment (Bio-Rad, Hercules, CA) and a semi-dry transfer apparatus (Hoefer) in conjunction with Hybond ECL membranes (Amersham Pharmacia, UK). Proteins were detected using enhanced chemiluminescence (ECL, Amersham Pharmacia, UK) following one hour incubations at room temperature with the respective primary and horseradish peroxidase-conjugated anti-mouse antibodies (Sigma, Poole, UK). The mouse anti-influenza hemagglutinin (HA) monoclonal HA-11 (Covance Research Products, Berkeley, CA) was used at 1 μg/ml for detection of HA-tagged Pds5. Cdc2 was detected using the mouse monoclonal antibody Y100 (generated by J. Gannon and kindly provided by H. Yamano).

Gel filtration chromatography

Chromatographic separation of *S. pombe* lysates was carried out using a superose-6™ column attached to an FPLC workstation (Amersham Pharmacia, UK). Cells from a 100 ml culture of the *pds5-HA* strain in mid-exponential growth were washed and resuspended in 300 μl FPLC buffer (20% glycerol, 20 mM Tris-Cl pH 7.5, 100 mM NaCl, 0.1 mM EDTA, 1 mM β-mercaptoethanol, 60 mM β-glycerophosphate, 0.1 mM sodium orthovanadate, 1 mM PMSF) with additional protease inhibitors (Complete™, Roche) and lysed by bead beating (3×30 seconds). After clearing by centrifugation (16,000 ***g***, 15 minutes) the lysate was loaded onto the column that had been pre-equilibrated with 50 ml FPLC buffer. The eluate was collected in 0.5 ml fractions and these were analysed by SDS-PAGE and immunoblotting. The column was calibrated using the standards: blue dextran (~2000 kDa), thyroglobin (670 kDa), apoferritin (443 kDa), β-amylase (200 kDa), BSA (66 kDa) and carbonic anhydrase (29 kDa).

Microscopy

Cells fixed in 3.8% formaldehyde were washed in phosphate-buffered saline and stained with 4′,6-diamidino-2-phenylindole (DAPI) before examination by fluorescence microscopy. Images were acquired using a Zeiss Axioskop microscope equipped with a Planapochromat 100× objective, an Axiocam cooled CCD camera and Axiovision software (Carl Zeiss Ltd, Welwyn Garden City, UK), and were assembled using Adobe PhotoShop. In some experiments living cells growing in EMM2 medium were stained by the addition of 5 μg/ml bis-benzimide (Hoechst 33342, Sigma) before examination by fluorescence microscopy. Visualisation of GFP-Swi6 in living cells embedded in 0.6% LMP agarose was performed at room temperature (approximately 22°C) as described elsewhere (Pidoux et al., 2000).

Results

S. *pombe pds5* is not essential for mitotic growth

BLAST (basic local alignment search tool) searches of the complete *S. pombe* genome using the *S. cerevisiae* Pds5 amino acid sequence as a query identified a single *S. pombe* gene significantly similar to *PDS5*. ProfileScan analysis of the sequence of the corresponding predicted 1205 amino acid residue *S. pombe* protein (SPAC110.02; accession number Q9HFF5) showed a good match to the bipartite nuclear localisation sequence (NLS) consensus at residues 1129-1146. Similar NLS motifs are present in the C-terminal regions of BIMD, Spo76 and *S. cerevisiae* Pds5 (van Heemst et al., 1999). Multiple sequence alignments showed that, over its entire length, the predicted *S. pombe* protein sequence displays 23% identity (45% similarity) to *S. cerevisiae* Pds5 (Fig. 1A), and is related to similar extents to *S. macrospora* Spo76, *A. nidulans* BIMD and the human Pds5 orthologue AS3 (Geck et al., 1999). Among these proteins, the sequence conservation is concentrated in four main blocks, with the intervening spacers being somewhat longer in Spo76 and BIMD than in the other members of the family (Fig. 1A). In recognition of this level of sequence conservation, and in deference to the pre-existing *S. cerevisiae* nomenclature, we refer to this *S. pombe* gene as *pds5*$^+$. We identified several partial matches to the HEAT motif in the *S. pombe* Pds5 protein, including one between residues 396 and 423. This sequence lies within a more extensive region of significant similarity between Pds5 (residues 287 to 423) and Mis4 (residues 784 to 918; data not shown).

The one-step gene disruption method was used in a ura4$^-$/ura4$^-$ diploid *S. pombe* strain to replace one copy of the entire *pds5* open reading frame with the *ura4*$^+$ selectable marker. After induction of meiosis and sporulation, microdissection of tetrads showed that the *pds5::ura4*$^+$ alleles segregated 2:2, indicating that, in contrast to its *S. cerevisiae* orthologue, *S. pombe pds5*$^+$ is not essential for mitotic growth. Microscopic examination of exponentially growing cells with the *pds5::ura4*$^+$ genotype (*pds5Δ*) showed that there were no

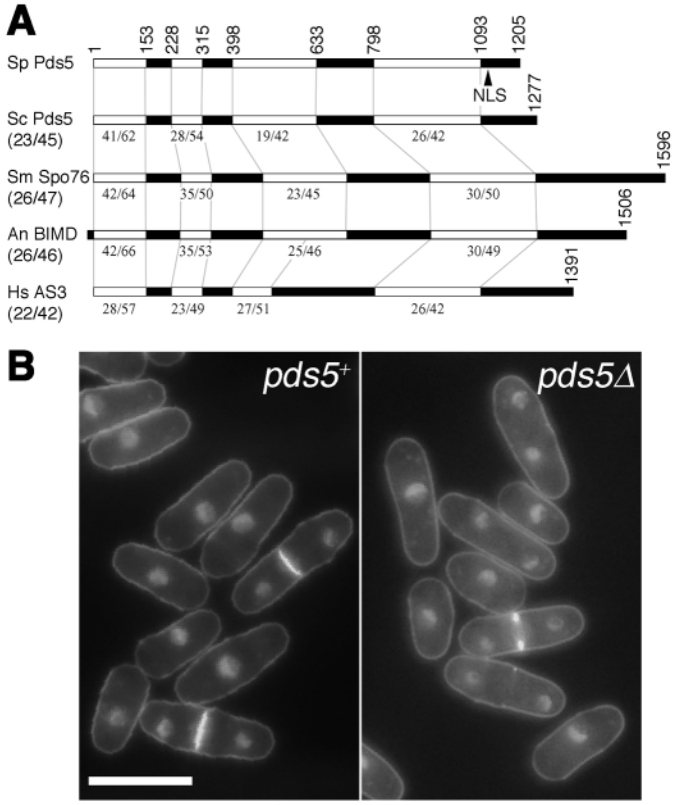

Fig. 1. The sole fission yeast Pds5 orthologue is non-essential for viability. (A) The predicted protein product of *S. pombe pds5* (SpPds5) with *S. cerevisiae* Pds5 (Sc Pds5), *S. macrospora* Spo76 (Sm Spo76), *A. nidulans* BIMD (An BIMD) and the human AS3 protein (Hs AS3). In each case the overall degree of relatedness to the *S. pombe* protein is indicated in parentheses (% identity/% similarity). Similarity between all five proteins is concentrated in the four regions filled in white, defined by the amino acid residue numbers shown above the *S. pombe* protein. The relatedness of each of these regions to the corresponding regions of the orthologous proteins is indicated (numbers below each conserved block; % identity/% similarity), along with the overall number of amino acid residues in each protein and the location of a predicted nuclear localisation sequence (NLS) in *S. pombe* Pds5. (B) Liquid cultures of HM123 (*pds5*$^+$) and *pds5Δ* strains were grown to mid-exponential phase and were stained with Hoechst 33342 to allow visualisation of DNA and septa by fluorescence microscopy. Bar, 10 μm.

gross abnormalities in cell growth or division associated with *pds5* deletion (Fig. 1B).

Deletion of *pds5* causes hypersensitivity to DNA damage

Since *A. nidulans bimD6* mutant cells display increased sensitivity to DNA damaging agents (Denison et al., 1993), we were interested to know if the same might be true of *S. pombe pds5Δ* cells. Exposure of *pds5Δ* cells and those of a *pds5*$^+$ control strain to UV showed that the *pds5Δ* strain is UV-hypersensitive, with a tenfold reduction in cell viability after exposure to 200 J/m^2 (Fig. 2A). Examination of the cells 12 hours after UV irradiation at 150 J/m^2 (a dose which only marginally reduced viability of the *pds5*$^+$ control) showed that most of the *pds5Δ* cells were highly elongated and had

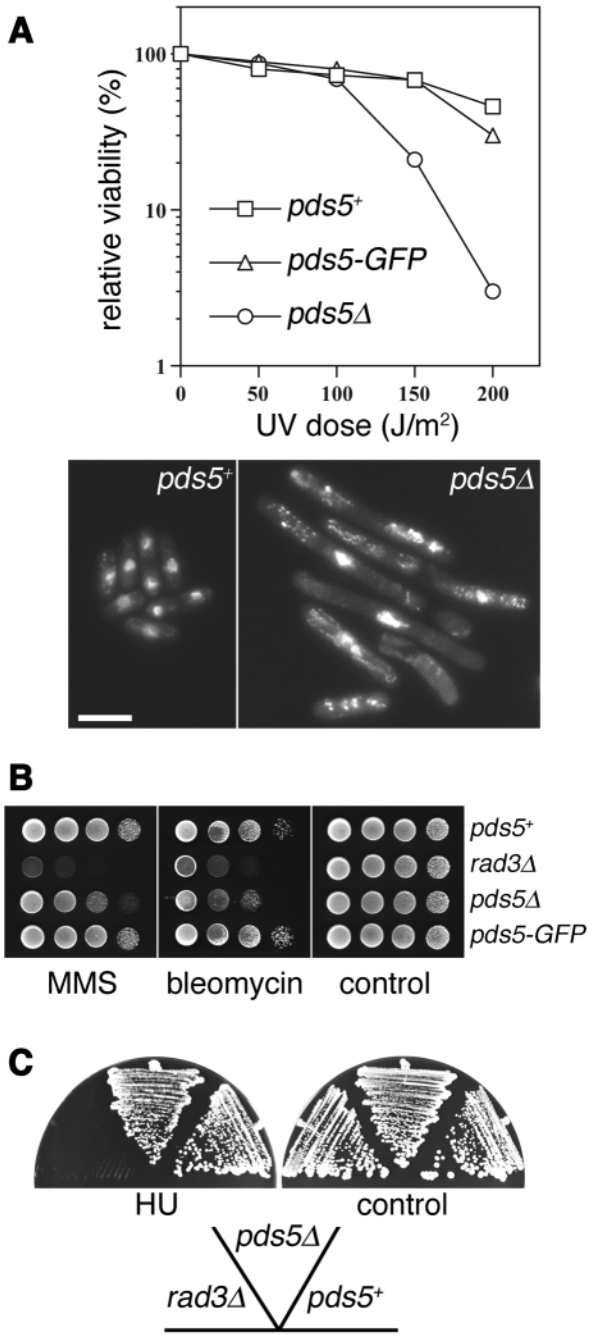

Fig. 2. *pds5Δ* cells are sensitive to DNA damaging agents, but not to inhibition of DNA replication. (A) Strains HM123 (*pds5*$^+$), *pds5-GFP* and *pds5Δ* were tested for sensitivity to UV. Colony numbers were counted after four days growth at 30°C following exposure to the indicated UV doses on YE agar plates, and were expressed as a percentage of the number of colonies seen after mock irradiation (upper panel). Cellular and nuclear morphologies of HM123 (*pds5*$^+$) and *pds5Δ* strains were determined by fluorescence microscopy of DAPI-stained cells 12 hours after exposure to 150 Jm^{-2} UV (lower panels; Bar, 10 μm). (B) Tenfold serial dilutions of HM123 (*pds5*$^+$) and the other strains indicated were spotted onto YE agar plates containing 0.005% MMS, 5 μg/ml bleomycin or neither drug (control). Plates were photographed after 3-5 days incubation at 30°C. (C) The strains indicated were streaked in the positions shown onto YE agar (control) or YE agar containing 10 mM HU. Plates were photographed after 4 days growth at 30°C.

fragmented and/or misshapen nuclei. The sensitivity of *pds5Δ* cells was not restricted to UV-induced DNA damage, as they were also mildly hypersensitive to the alkylating agent methyl methanesulphonate (MMS) and the radiomimetic agent bleomycin (Fig. 2B). While this sensitivity was significant, it was not as extreme as that seen in a strain lacking the checkpoint signalling kinase Rad3 (*rad3Δ*; Fig. 2B).

Mutants defective in the establishment of sister chromatid cohesion or in elements of checkpoint signalling have been shown in many cases to lose viability when DNA replication is inhibited. However, in contrast to their sensitivity to DNA damaging agents, *pds5Δ* cells were not sensitive to hydroxyurea (which inhibits ribonucleotide reductase and hence DNA replication), in comparison with those of a *rad3Δ* strain (Fig. 2C).

Pds5 is required for maintenance of viability when mitosis is arrested

S. cerevisiae pds5 mutants show a characteristic loss of viability during arrest in mitosis, and it was therefore of interest to determine if the same is true of the *S. pombe pds5Δ* strain. In comparison with a *pds5*$^+$ strain, *pds5Δ* cells were hypersensitive to the spindle poison thiabendazole (TBZ; Fig. 3A) and deletion of *pds5* showed synthetic lethality with the *nda3-KM311* β tubulin mutation (Hiraoka et al., 1984) at 23°C, at which temperature the cold-sensitive *nda3-KM311* single mutant is still able to grow (Fig. 3B). These data suggest that *pds5* is involved in maintenance of viability during delayed progression through mitotic metaphase. In order to define the *pds5Δ* defect more precisely, release from an *nda3-KM311*-induced metaphase block was monitored by microscopy of *pds5*$^+$ and *pds5Δ* cells. By 9 minutes after release most of the *pds5*$^+$ cells had entered anaphase with two apparently equal daughter nuclei (Fig. 3C). Under the same conditions the *pds5Δ* cells appeared to enter anaphase on schedule, but showed an unusually high proportion of cells with lagging chromosomes (Fig. 3C). At 2 hours after release these cells showed a variety of apparently lethal abnormalities, including total failure of chromosome segregation and the 'cut' (cell untimely torn) phenotype (data not shown). We conclude that failure to complete mitosis probably accounts for the observed genetic interaction between *pds5* deletion and *nda3-KM311*, and for the sensitivity of the *pds5Δ* strain to TBZ.

Sensitivity of *S. cerevisiae pds5* mutants to anti-microtubule agents has been ascribed to their failure to maintain sister chromatid cohesion during mid-mitotic arrest (Hartman et al., 2000; Panizza et al., 2000). Sister centromere separation in living *S. pombe* cells can be monitored conveniently by the use

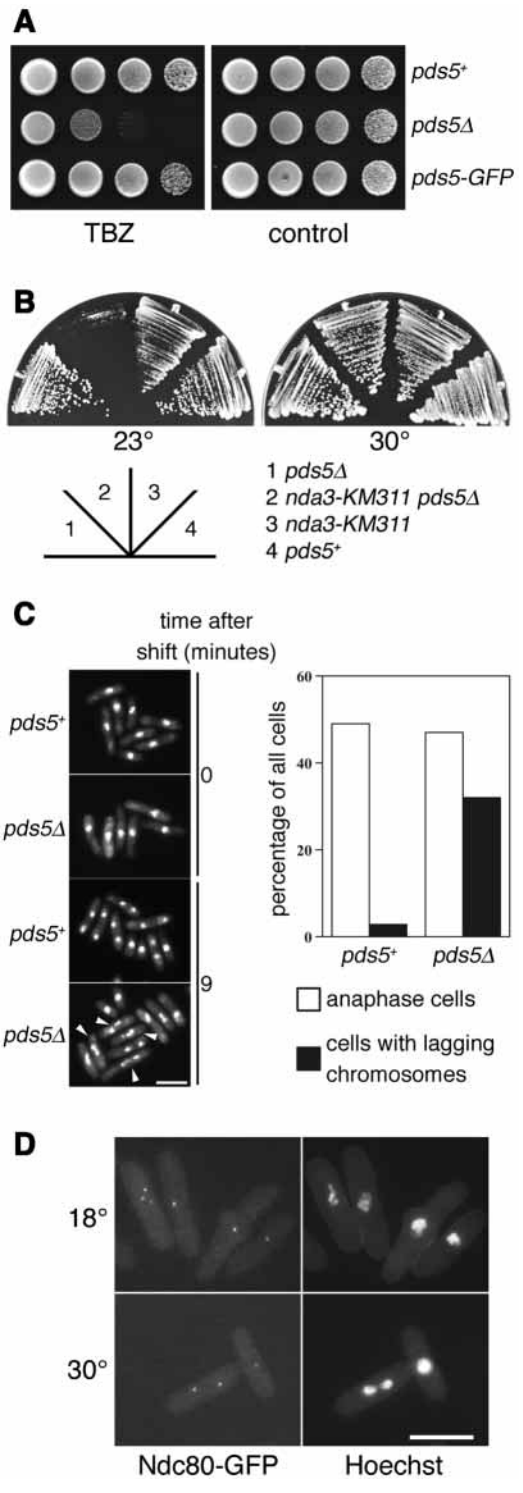

Fig. 3. *pds5Δ* cells are sensitive to delayed progression through mitosis, but do not undergo precocious sister chromatid separation during metaphase arrest. (A) Tenfold serial dilutions of HM123 (*pds5*$^+$), *pds5Δ* and *pds5-GFP* strains were spotted onto YE agar containing 20 μg/ml TBZ or no drug (control). Plates were photographed after 3-5 days incubation at 30°C. (B) HM123 (*pds5*$^+$) and the other strains indicated were streaked in parallel onto YE agar plates and were photographed after 5 days incubation at 23°C or 30°C, as indicated. (C) Micrographs of formaldehyde fixed, DAPI stained *nda3-KM311* (*pds5*$^+$) and *nda3-KM311 pds5Δ* (*pds5Δ*) cells before (0 minutes) and 9 minutes after shifting to 36°C to release from a metaphase arrest, imposed previously by holding the cells at 20°C for 8 hours. Examples of anaphase cells with lagging chromosomes are indicated by arrowheads. The percentages of total anaphase cells and anaphase cells with lagging chromosomes 9 minutes after release are indicated graphically on the right. (D) The *nda3-KM311 ndc80-GFP pds5Δ* strain was incubated in EMM2 medium at 30°C or shifted to 18°C for 12 hours. Fluorescence micrographs of living cells were acquired after staining with Hoechst 33342, revealing green fluorescence (Ndc80-GFP) and DNA (Hoechst) in the same field, as indicated. Bars, 10 μm.

of a strain expressing a green fluorescent protein (GFP)-tagged version of the kinetochore component Ndc80 (Wigge and Kilmartin, 2001). Ndc80-GFP appears as a single fluorescent spot in interphase cells, while in anaphase the clustered kinetochores are seen as two spots, one in each daughter nucleus. This pattern of Ndc80-GFP distribution was seen in *nda3-KM311 pds5Δ* cells grown at the permissive temperature of 30°C (Fig. 3D). When this strain was shifted to the restrictive temperature of 18°C to induce arrest in a metaphase, most cells (95%) still showed a single Ndc80-GFP spot, indicating that the sister centromeres were clustered. The remaining cells had three well-defined masses of condensed chromatin, presumably corresponding to the three *S. pombe* chromosomes, with an Ndc80-GFP spot associated with each (Fig. 3D). Of a total of 500 cells examined, none with more than three Ndc80-GFP spots was seen. Thus, in contrast to the corresponding *S. cerevisiae* mutant, *S. pombe pds5Δ* cells showed no indication of premature sister centromere separation during metaphase arrest.

Elevated rate of chromosome loss on deletion of *pds5*

Given the chromosome segregation defects observed on release of *pds5Δ* cells from metaphase arrest, we reasoned that Pds5 might also be required to ensure the normal fidelity of chromosome segregation during unperturbed mitosis. To address this point, *pds5*$^+$ and *pds5Δ* strains containing a non-essential minichromosome (Ch16) carrying an adenine biosynthetic marker were used to measure rates of chromosome loss (Fig. 4A). This assay showed that spontaneous loss of the minichromosome was 30-fold more frequent in the *pds5Δ* strain in comparison with the *pds5*$^+$ control (mean loss rates were 0.00714 and 0.00024 per

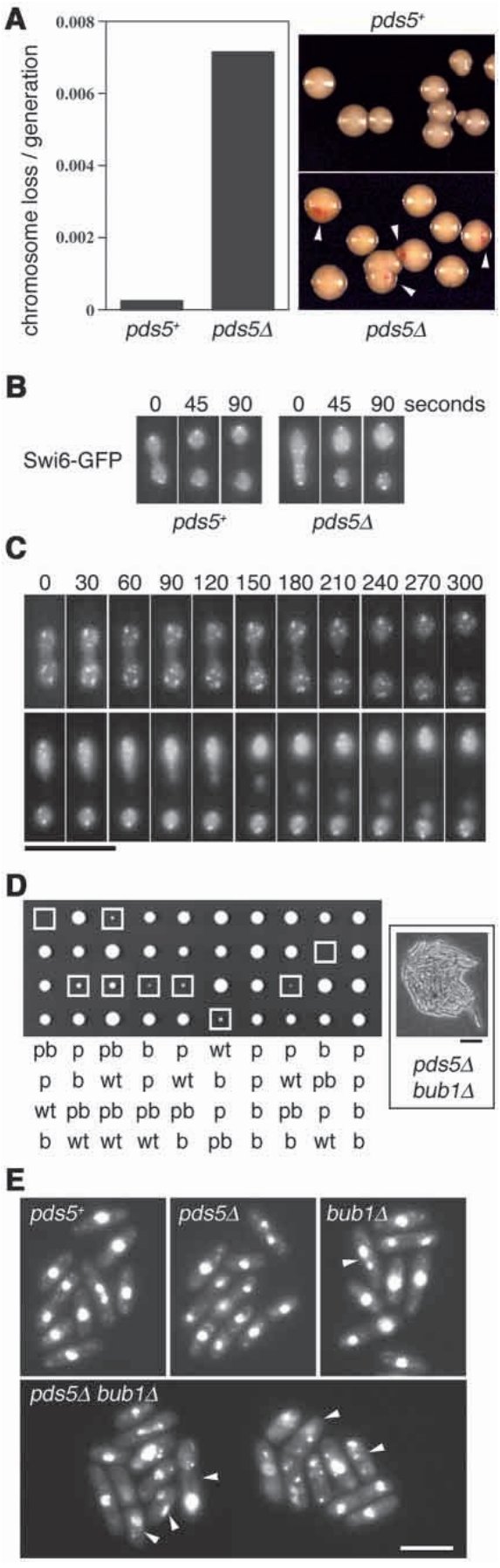

Fig. 4. Deletion of *pds5* leads to an increased chromosome segregation failure rate. (A) Rates of mini-chromosome loss were calculated for strains HM248 (*pds5*$^+$) and *pds5Δ Ch16* (*pds5Δ*) as described in Materials and Methods and are expressed as mean chromosome loss per generation. Arrowheads in the right-hand panels indicate examples of ade$^-$ sectored colonies indicative of chromosome loss. (B) Living *GFP-swi6* (*pds5*$^+$) and *GFP-swi6 pds5Δ* (*pds5Δ*) cells were observed by green fluorescence microscopy. In each case a series of three images of a single cell progressing through early anaphase is shown; images were acquired at the time points indicated. (C) Visualisation of lagging chromosomes in *pds5Δ* cells. Individual *GFP-swi6 pds5Δ* cells were observed as in (B), over a 5 minute period, with images collected every 30 seconds. Bar, 10 μm. (D) Genetic interaction between *pds5* and *bub1*. Ten tetrads derived from a diploid *h*$^+$/*h*$^-$ *pds5:ura4*$^+$/*pds5*$^+$ *bub1::LEU2*/*bub1*$^+$ *ura4-D18/ura4-DS/E leu1-32/leu1-32* strain were microdissected onto YE agar and the resulting colonies were photographed after 4 days growth at 30°C. The genotypes of the segregants were determined by replica plating and are indicated schematically below (wt, *pds5*$^+$ *bub1*$^+$; p, *pds5:ura4*$^+$; b, *bub1::LEU2*; pb, *pds5:ura4*$^+$ *bub1::LEU2*; the latter is also indicated by white boxes in the upper panel). The inset panel shows a micrograph of a representative *pds5:ura4*$^+$ *bub1::LEU2* colony taken at the same time. Bar, 20 μm. (E) Slow growth of *pds5Δ bub1Δ* cells is associated with chromosome segregation defects. Fluorescence micrographs of formaldehyde fixed, DAPI-stained cells from exponentially growing YE liquid cultures of HM123 (*pds5*$^+$) and the indicated strains. Cells exhibiting abnormal chromosome segregation are indicated (arrowheads).

generation, respectively). We conclude that, while not essential, *pds5*$^+$ makes an important contribution to maintenance of genome stability in *S. pombe*.

Although the gross nuclear morphology of most *pds5Δ* cells appeared normal (Fig. 1B), we were interested to see if the elevated rate of mini-chromosome loss would be reflected in chromosome segregation defects as scored by microscopy. To address this point, *pds5Δ* and *pds5*$^+$ strains were constructed containing an integrated GFP-tagged *swi6* gene. Like the endogenous chromodomain protein Swi6, GFP-Swi6 localizes to the nucleus and is concentrated at the heterochromatic centromeres and telomeres (Pidoux et al., 2000). Anaphase chromosome separation, monitored in living cells by GFP-Swi6 fluorescence microscopy, appeared normal in the *pds5*$^+$ background, as well as in the majority of *pds5Δ* cells. Abnormal anaphase progression was nonetheless detectable in approximately 5% of the *pds5Δ* cells, but not in the *pds5*$^+$ control (Fig. 4B,C). In some cells this took the form of segregation, with apparently normal kinetics, of two unequal masses of GFP-Swi6 (Fig. 4B). In other *pds5Δ* cells an extended bridge of GFP-Swi6 persisted for some time between the presumptive daughter nuclei (Fig. 4C, upper panels), while still others contained discrete centers of GFP-Swi6 fluorescence, presumably corresponding to entire lagging chromosomes (Fig. 4C, lower panels). Chromosome segregation defects at the frequencies seen would be sufficient to account for the elevated rate of minichromosome loss in *pds5Δ* cells.

One possible explanation for the observed mitotic defects in *pds5Δ* cells would be that, in the absence of Pds5, some aspect of centromere function or spindle microtubule attachment is defective in a significant proportion of cells. To address this possibility, the effect of combining the *pds5* deletion with deletion of the *bub1* spindle checkpoint gene (Bernard et al., 1998) was investigated. In the absence of *bub1*, cells with centromeric defects fail to delay the onset of anaphase appropriately and suffer catastrophic chromosome mis-segregation. Tetrad dissection following sporulation of a *pds5Δ/pds5*$^+$ *bub1Δ/bub1*$^+$ diploid strain showed that *pds5Δ bub1Δ* double mutants grew much more slowly than the equivalent single mutants (Fig. 4D). Examination of DAPI stained samples from liquid cultures showed that *bub1Δ* cells suffered chromosome mis-segregation events (Fig. 4E), as reported previously (Bernard et al., 1998). These were more frequent than those seen in *pds5Δ* cells, but were not sufficient to cause a significant growth disadvantage such as that seen in *pds5Δ bub1Δ* mutants (Fig. 4D). The growth disadvantage in the latter was associated with a variety of chromosome mis-segregation events (Fig. 4E). Interestingly, no such genetic interaction was seen between *pds5Δ* and deletion of *mad2*, another spindle checkpoint gene (data not shown).

Meiosis is frequently abnormal in the absence of *pds5*

In *S. macrospora*, Spo76 is required for sister chromatid cohesion both in mitosis and in meiosis. Having established that Pds5, the only protein in *S. pombe* significantly related to Spo76, has a role in the mitotic cell cycle, we therefore made a preliminary investigation of the possibility that Pds5 might also have a role in meiosis. Induction of meiosis and sporulation in a homozygous *pds5Δ* diploid strain gave rise to

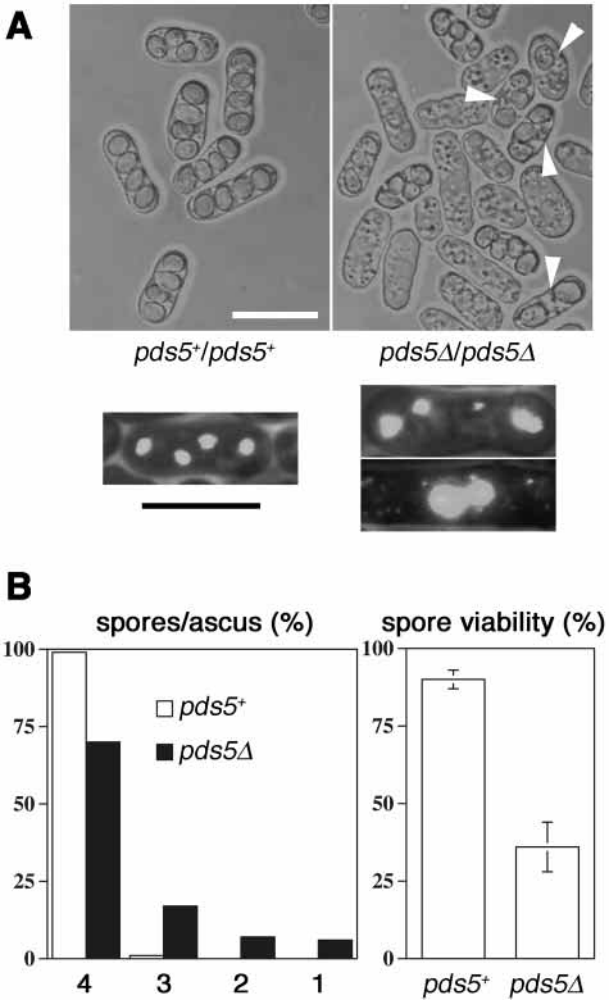

Fig. 5. Meiotic defects in the absence of Pds5. (A) Phase-contrast micrographs of living cells (upper panels) and fluorescence micrographs of DAPI-stained, formaldehyde-fixed cells (lower panels) of sporulating 428h/429h (*pds5*$^+$/*pds5*$^+$) and *pds5Δ/pds5Δ* strains are shown, as indicated. Bars, 10 μm. (B) Quantification of the sporulation defect in *pds5Δ/pds5Δ* progeny. The percentages of all asci containing four, three, two or one spores, and the overall spore viabilities of 428h/429h (*pds5*$^+$) and *pds5Δ/pds5Δ* (*pds5Δ*) strains are shown, as indicated (error bars represent one standard deviation in the right-hand panel; the mean of three separate measurements is shown).

asci, 30% of which had fewer than four spores, which were in most cases misshapen and abnormally sized and had substantially reduced viability (Fig. 5). The DNA content of these abnormal spores was frequently either greater or less than that of normal haploid spores (Fig. 5A, lower panels). By contrast, atypical asci of this sort represented <1% of those formed in parallel by a *pds5*$^+$/*pds5*$^+$ diploid strain. Completion of meiosis and/or sporulation at the normal frequency thus depends at some level on *pds5*$^+$ function.

Characterisation of Pds5 protein in *S. pombe*

Targeted recombination was used to add an HA epitope tag sequence to the 3′ end of the *pds5* open reading frame in its

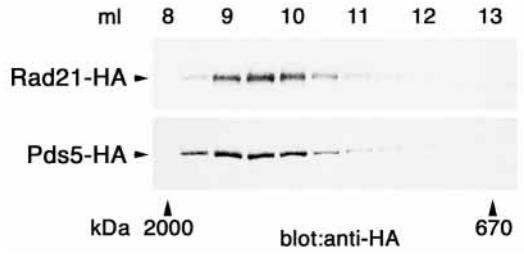

Fig. 6. Rad21 and Pds5 are present in high molecular weight complexes of similar sizes. The sizes of soluble Rad21-HA and Pds5-HA were estimated in parallel by gel filtration chromatography as described in Materials and Methods and cell extracts from the *rad21-HA* and *pds5-HA* strains. Samples of each 0.5 ml Superose 6 column fraction were processed for immunoblotting with an anti-HA antibody. The elution volume (ml) of each fraction is shown above the blots. The positions at which dextran blue (void volume; ~2000 kDa) and thyroglobin (670 kDa) migrated are indicated. The remaining smaller size fractions did not contain significant amounts of either HA-tagged protein.

normal chromosomal context, generating the *pds5-HA* strain (see Materials and Methods). Immunoblotting of *pds5-HA* whole cell lysates with an anti-HA antibody showed a single protein band of approximately 140 kDa, consistent with the predicted relative molecular mass for Pds5 of 138874 (Fig. 6; and data not shown). Immunoblotting of anti-PDS5 immunoprecipitates from human cells has been used to demonstrate an interaction between PDS5 and cohesin subunits, although most PDS5 was not found to be stably associated with cohesin as judged by sucrose gradient fractionation of cell extracts (Sumara et al., 2000). No size fractionation data have been published to date for *S. cerevisiae* Pds5 or any of its fungal orthologues, however. We therefore used gel filtration chromatography to estimate the apparent size of *S. pombe* Pds5 in a cell lysate prepared from the *pds5-HA* strain (Fig. 6). Under the conditions used, the HA-tagged Pds5 migrated as a single peak with an apparent size between 670 and 2000 kDa. Parallel fractionation of an extract from a *rad21-HA* strain showed that the Rad21-HA protein (and, by extension, other previously characterized cohesin components) was also present in a single peak with a similar size distribution to that seen for Pds5-HA.

The relationship between Pds5 and cohesin

To monitor the localisation of Pds5 in living cells, the one step gene replacement method was used to generate a strain (*pds5-GFP*) encoding a C-terminally GFP tagged version of Pds5. The GFP-tagged protein appeared to be functional as judged by the lack of hypersensitivity to UV of the *pds5-GFP* strain compared with *pds5Δ* (Fig. 2A,B). Examination of living *pds5-GFP* cells by fluorescence microscopy showed that Pds5-GFP (and, by inference Pds5) was predominantly localised to the nucleus, within which it gave a diffusely speckled signal (Fig. 7A). There were no obvious differences in this pattern among cells at different cell cycle stages, and in *nda3-KM311* cells arrested in a metaphase-like state by incubation at the restrictive temperature of 18°C for 12 hours the Pds5-GFP signal co-localised with condensed chromosomes.

Localisation of Pds5 to chromatin in *S. cerevisiae* is dependent upon the integrity of the Scc1/Mcd1 cohesin component (Hartman et al., 2000; Panizza et al., 2000). To see if the same might be true of the orthologous *S. pombe* proteins,

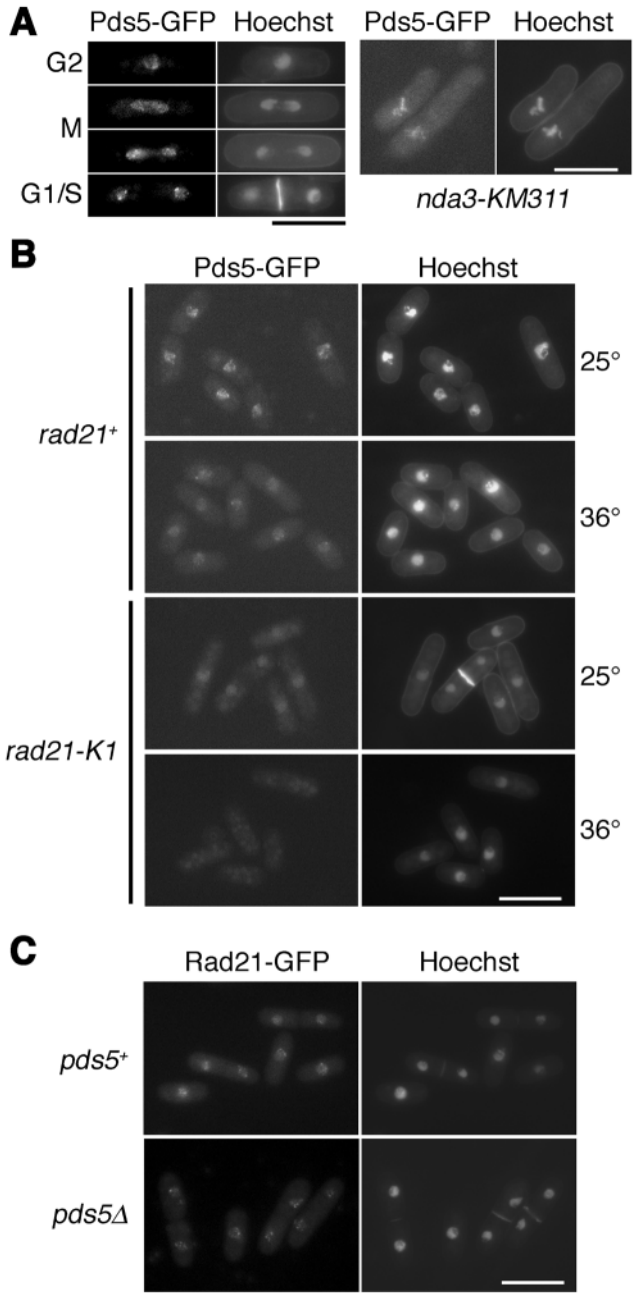

Fig. 7. Nuclear localisation of Pds5 is cohesin-dependent, and cohesin localisation is altered in the absence of Pds5. (A,B) Fluorescence micrographs showing Pds5-GFP and DNA (Hoechst 33342) localisation in living cells. (A) Left panels show examples from an asynchronous culture of *pds5-GFP* cells at the cell cycle stages indicated. Right panels show metaphase arrested *nda3-KM311 pds5-GFP* cells after 12 hours incubation at 18°C. (B) *pds5-GFP* (*rad21*$^{+}$) and *rad21-K1 pds5-GFP* (*rad21-K1*) cells grown at 25°C or shifted to 36°C for 3 hours, as indicated. (C) Fluorescence micrographs showing Rad21-GFP and DNA (Hoechst 33342) in living *rad21-GFP* (*pds5*$^{+}$) and *pds5Δ rad21-GFP* cells (*pds5Δ*), as indicated. Bars, 10 μm.

the localisation of Pds5-GFP was monitored in a temperature-sensitive *rad21-K1* strain (Fig. 7B). At the permissive temperature of 25°C, Pds5-GFP was again predominantly nuclear, but after inactivation of the Rad21 cohesin component by shifting to the restrictive temperature of 36°C the Pds5-GFP signal was diffusely localised throughout the cell. No such change in localisation was seen on shifting a *pds5-GFP* (*rad21*$^+$) strain from 25°C to 36°C (Fig. 7B). Thus Pds5 localisation to the nucleus is cohesin-dependent in *S. pombe*, as it is in *S. cerevisiae*. By contrast, Rad21-GFP remained in the nuclear compartment on deletion of *pds5*, although in *pds5Δ rad21-GFP* cells the Rad21-GFP appeared more punctate than it did in *pds5*$^+$ cells (Fig. 7C).

To investigate further this apparent relationship between pds5 and cohesin, the meiotic progeny of a diploid *rad21-K1 pds5Δ* strain (Table 1) were characterised following tetrad microdissection (Fig. 8A). From 102 tetrads, the numbers of *pds5*$^+$ *rad21*$^+$, *pds5*$^+$ *rad21-K1* and *pds5::LEU2 rad21*$^+$ segregant colonies visible after 5 days growth at 25°C were 77, 45 and 78, respectively. These numbers are lower than the 102 that would be expected for independently segregating markers, and indicate that there was an overall loss of spore viability attributable to heterozygosity at the *pds5* and *rad21* loci in the diploid. Nonetheless, haploid segregants bearing either the *rad21-K1* or the *pds5::LEU2* allele were able to grow and form colonies reasonably efficiently. By contrast, no *rad21-K1 pds5::LEU2* segregant colonies were visible after 7 days growth. In many cases the positions occupied by spores of this genotype could be deduced from the genotypes of the other segregants. Microscopic examination showed that these *rad21-K1 pds5::LEU2* cells were highly elongated, suggesting that partial loss of *rad21* function in the absence of *pds5* leads to a failure of cell cycle progression (Fig. 8A).

Further genetic interactions between the *pds5* deletion and genes encoding components of the sister chromatid cohesion pathway were sought. *S. pombe* Mis4 is a cohesin loading factor/adherin orthologous to *S. cerevisiae* Scc2. Introduction of the temperature sensitive *mis4-242* mutation into a *pds5Δ* background revealed a synthetic lethality phenotype at 28°C, at which temperature each of the corresponding single mutants grew relatively normally (Fig. 8B). Reducing the temperature to 25°C allowed the *pds5Δ mis4-242* cells to grow, albeit slowly. On microscopic examination these cells showed a variety of aberrant morphologies indicative of cell cycle defects, including extensive elongation and chromosome mis-segregation (Fig. 8B, lower panel). No such defects were seen in the single *mis4-242* mutant grown at the same temperature. Thus *pds5* can be linked genetically both to cohesin itself and to a cohesin loading factor.

Discussion

Pds5-related proteins have previously been implicated in sister chromatid cohesion in organisms as diverse as fungi and vertebrates. Loss of function of *PDS5*/*SPO76/bimD* in distantly related simple eukaryotes is nonetheless associated with a marked variety of phenotypes, encompassing complete

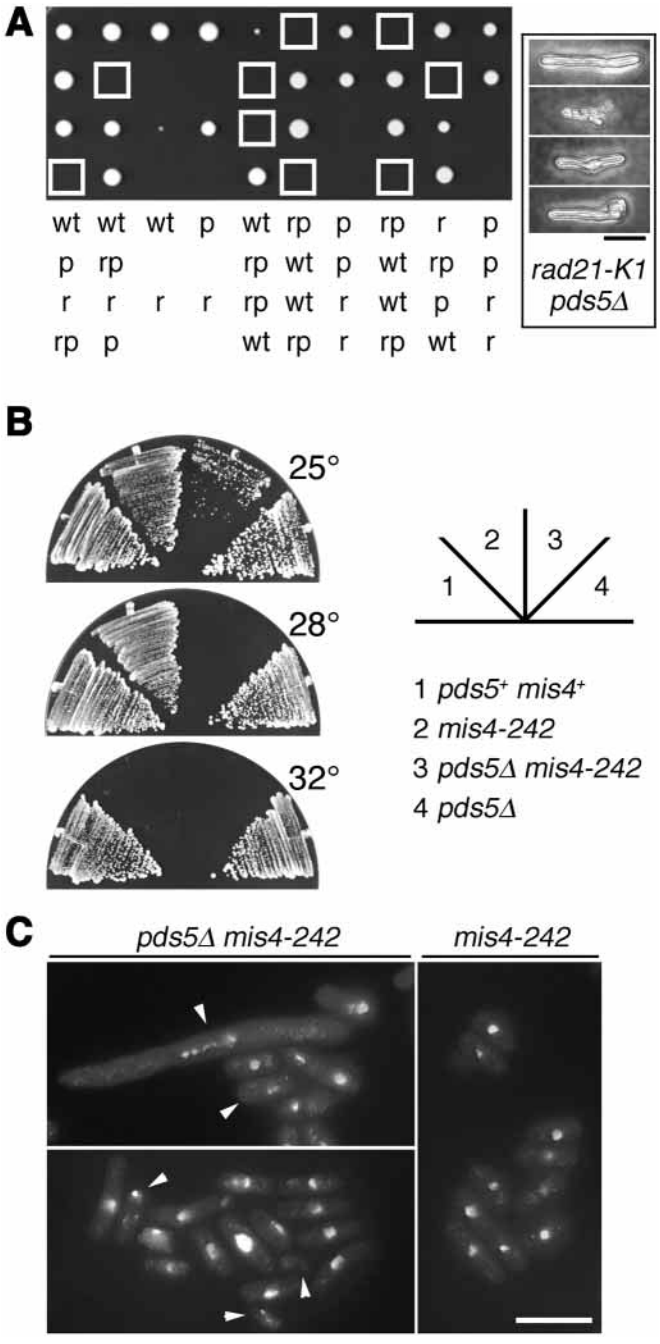

Fig. 8. Genetic interactions between *pds5*, *rad21* and *mis4*. (A) Ten tetrads derived from the diploid strain *rad21-K1 pds5Δ* (*h*$^+$ *h*$^-$ *rad21-K1:ura4/rad21*$^+$ *pds5::LEU2/pds5*$^+$ *ade6-M210/ade6-M216 leu1-32/leu1-32 ura4-D18/ura4-D18*) were microdissected onto YE agar, and the resulting colonies were photographed after 5 days growth at 30°C. The genotypes of the segregants were determined by replica plating and are indicated schematically below (wt, *pds5*$^+$ *rad21*$^+$; p, *pds5::LEU2*; r, *rad21-K1*:*ura4*$^+$; rp, *rad21-K1*:*ura4*$^+$ *pds5::LEU2*; the latter are also indicated by white boxes in the upper panel). The terminal phenotype of *rad21-K1*:*ura4*$^+$ *pds5::LEU2* segregants was determined by microscopic examination of the cells *in situ* after 5 days growth at 30°C. Four representative examples are shown in the inset panel on the right. (B) HM123 (*pds5*$^+$ *mis4*$^+$) and the other strains indicated were streaked in parallel onto YE agar plates and were photographed after incubation for 3-5 days at the temperatures indicated. (C) fluorescence micrographs of formaldehyde fixed, DAPI stained *pds5Δ mis4-242* and *mis4-242* cells grown at 25°C. Bars, 10 μm.

failure of mitotic chromosome segregation as well as much more subtle mitotic and meiotic defects. In order to clarify common functions of these proteins, we have investigated the localisation and function of the product of *pds5*, the sole representative of the *PDS5*/*SPO76/bimD* family in *S. pombe*. The primary amino acid sequences of Pds5 and its orthologues are related to each other to similar degrees throughout their length, with particularly strong conservation in the N-terminal ~150 amino acid residues (Fig. 1A).

In some respects, *S. pombe pds5*$^{+}$ more closely resembles *S. macrospora SPO76* than *S. cerevisiae PDS5* or *A. nidulans bimD*. Specifically, the *S. pombe* gene is dispensable for mitotic growth but is required for the efficient completion of meiosis and sporulation (Figs 1, 5). Pds5 was found previously to be required for chromosome condensation as well as cohesion in *S. cerevisiae* (Hartman et al., 2000), but we find no indication that *S. pombe* Pds5 is required for the chromosome condensation seen in metaphase arrested cells (Fig. 3D). If the link between cohesion and condensation that has been described in *S. cerevisiae* (Guacci et al., 1997) also operates in the fission yeast, the competence of *pds5Δ* cells for chromosome condensation would be consistent with their lack of overt cohesion defects (Fig. 3). However, Mis4, which is required for sister chromatid cohesion in *S. pombe*, is not required for condensation (Furuya et al., 1998), suggesting that any such link may not be straightforward. Indeed, it has been suggested that, in *Xenopus*, cohesin may not be involved in chromosome condensation at all (Losada et al., 1998). An involvement in chromosome condensation in *S. cerevisiae* but not in *S. pombe* might explain why Pds5 is essential for viability in the former but not the latter.

What then might be the mitotic role of *S. pombe* Pds5? Despite the lack of precocious sister chromatid separation in *pds5Δ* cells under the conditions tested here, a number of lines of evidence point towards an intimate connection between Pds5 and the cohesion process. First, like its budding yeast counterpart, *S. pombe* Pds5 localises to nuclear foci in a manner that is dependent on cohesin function (Fig. 7A-C). The constitutive localisation of Pds5 to this nuclear compartment throughout the *S. pombe* cell cycle is reminiscent of the behaviour of the Rad21 cohesin (Tomonaga et al., 2000) and Mis4 adherin (Furuya et al., 1998). The majority of cohesin remains associated with chromatin throughout the mitotic cell cycle in *S. pombe*, in contrast to the situation in budding yeast, where Scc1/Mcd1 cleavage at the onset of anaphase is associated with dissociation of cohesin and Pds5 from the chromosomes (Guacci et al., 1997; Hartman et al., 2000; Michaelis et al., 1997; Panizza et al., 2000; Toth et al., 1999). The persistence of Pds5-GFP in cells at all stages of mitosis (Fig. 7A) suggests that, unlike Scc1/Rad21, Pds5 may not be regulated by proteolysis. Disappearance of Pds5-GFP from the nucleus on inactivation of Rad21 (Fig. 7C) suggests that the putative bipartite NLS in Pds5 (Fig. 1A) is insufficient to confer constitutive nuclear localisation. In the absence of functional cohesin, Pds5 may be subject to nuclear export or degradation; distinction between these possibilities awaits further investigation.

A role for *S. pombe* Pds5 in chromatid cohesion would also be consistent with the genetic interactions between *pds5*, *rad21* and *mis4* (Fig. 8). The observed lack of hypersensitivity of *pds5Δ* cells to HU (Fig. 2C) suggests that *pds5* may not be required for the establishment of cohesion in S phase, in contrast to *mis4*, which when mutated confers HU hypersensitivity (Furuya et al., 1998). A role in cohesion could also be suggested by the sensitivity of *pds5Δ* cells to DNA damage (Fig. 2). Mutation of other genes involved in the establishment or maintenance of cohesion has previously been shown to lead to DNA damage sensitivity (Birkenbihl and Subramani, 1992; Denison et al., 1993; Furuya et al., 1998; Sjögren and Nasmyth, 2001). The elongation of *pds5Δ* cells seen after UV irradiation (Fig. 2A) suggests that cell cycle checkpoint responses to UV-induced DNA damage are established in the absence of *pds5*, but that some aspect of DNA repair or cell cycle resumption is defective, accounting for the observed increase in UV sensitivity. A general role for Pds5 in cell cycle resumption seems unlikely, however, as G2 arrest for up to 6 hours in a *cdc25-22 pds5::ura4*$^{+}$ strain was not accompanied by any significant loss of viability (data not shown). Instead, a role for Pds5 in promoting repair of a variety of DNA lesions seems more likely (Fig. 2). This function could be an indirect consequence of a primary involvement of Pds5 in cohesion.

In line with the proposed connection between Pds5 and cohesion in *S. pombe*, soluble Pds5 was present in a high molecular weight complex similar in size to that containing the Rad21 cohesin component (Fig. 6). This is consistent with the behaviour of human PDS5, which could be co-immunoprecipitated with cohesin components from crude cell lysates, although it was exclusively localised to size fractions smaller than those containing cohesin when lysates were separated by sucrose density gradient centrifugation (Sumara et al., 2000). Interestingly, size fractionation of *pds5-HA* lysates in the absence of phosphatase inhibitors yielded a Pds5-HA peak with a much smaller average size, consistent with that expected for the monomeric protein (data not shown). This suggests that retention of Pds5 in a high molecular weight complex, perhaps including cohesin itself, depends on the maintenance of phosphorylation of one or more proteins. Despite this apparent co-migration, we were unable to co-immunoprecipitate known cohesin components reproducibly with Pds5-HA, or to precipitate Pds5-HA with an anti-Rad21 antibody (data not shown). Any interaction between Pds5 and cohesin therefore appears quite labile in soluble extracts. However, our data do not rule out the possibility that such an interaction might be more stable in the context of chromatin-associated cohesin.

In the mitotic cycle, *pds5Δ* cells had an elevated rate of chromosome loss and lagging chromosomes were readily detected (Fig. 4). These cells were also unusually vulnerable to arrest at metaphase, as judged by TBZ sensitivity and synthetic lethality with *nda3-KM311* at 23°C (Fig. 3). Microscopic examination of *pds5Δ* cells released from an *nda3-KM311* arrest suggested that chromosome segregation was frequently grossly abnormal under these circumstances. In the absence of any evidence for precocious sister separation, it is still possible that these observations reflect altered cohesion. For example, Pds5 may be required for the correct localisation of cohesin to specific chromosomal sites, or for the inhibition of excessive cohesin loading. These possibilities would be consistent with our observation that Rad21-GFP remains associated with chromatin in the absence of Pds5, although the precise pattern of its chromatin localisation appears subtly different (Fig. 7C). In this case the frequent failure of *pds5Δ*

cells to complete mitosis properly after metaphase delay (Fig. 3C) could be the result of anaphase progression without complete loss of sister chromatid cohesion. Similar defects, occurring at a lower frequency, could explain the 30-fold elevation in minichromosome loss and the presence of lagging chromosomes in *pds5Δ* cells (Fig. 4). As this aspect of the *pds5Δ* phenotype is particularly marked after a metaphase delay, it would appear that the putative regulatory role of Pds5 is more important during mitosis than it is in interphase. Analogous defects in meiosis I and/or II could explain the observed defects in spore formation (Fig. 5).

The sensitivity of *pds5Δ* cells to metaphase arrest does not appear to reflect a loss of spindle checkpoint integrity, since *nda3-KM311 pds5Δ* cells were able to arrest in a metaphase-like state on being shifted to the restrictive temperature (Fig. 3C,D). The potent genetic interaction observed between *pds5* and *bub1* (Fig. 4D,E) could suggest that the spindle checkpoint is at least partially activated in *pds5Δ* cells in the absence of any additional perturbation. If this is the case Pds5, through its putative role in 'fine tuning' sister chromatid cohesion, may be required for the efficient establishment of bipolar attachments of chromosomes to spindle microtubules. Interestingly, we found no equivalent genetic interaction between *pds5* and *mad2*, while the mitotic delay in *S. pombe* cohesin mutants was reported to be *mad2*-dependent (Tomonaga et al., 2000). A recent study demonstrated that, in addition to its spindle checkpoint function, Bub1 is required for centromeric cohesion during meiosis (Bernard et al., 2001). The genetic interaction between *pds5* and *bub1* (Fig. 4) could therefore indicate that both are also involved in mitotic cohesion.

Investigation of cohesin-related components in *S. pombe* should prove complementary to studies in *S. cerevisiae* with respect to understanding chromatid cohesion and its regulation in other organisms, as the overall organisation of mitosis in the two yeasts differs in several respects (Russell and Nurse, 1986). Indeed, significant differences between these species in terms of cohesin composition and proteolysis have been described recently (Tomonaga et al., 2000). Specifically, Psc3 (the *S. pombe* orthologue of Scc3) is not stably associated with cohesin, and only a minor fraction of Rad21 is subject to proteolysis at the onset of anaphase. Genetic approaches in distantly related simple eukaryotes, combined with biochemical investigations in these and other systems, should eventually provide a comprehensive understanding of sister chromatid cohesion and its regulation.

We are grateful to Mitsuhiro Yanagida and Takashi Toda for valuable advice and provision of strains, to John Kilmartin, Tony Carr, Robin Allshire, Jean-Paul Javerzat and Hideo Ikeda for additional strains, and to Ian Hickson and other members of the ICRF Molecular Oncology Laboratory for their advice and comments on the manuscript. This work was supported by the Imperial Cancer Research Fund, the Association of Commonwealth Universities (scholarship to R.L.R.) and the Association for International Cancer Research.

References

Ausubel, F. M., Brent, R., Kingston, R. E., Moore, D. D., Seidman, J. G., Smith, J. A. and Struhl, K. (1995). *Current Protocols in Molecular Biology*. New York: John Wiley & Sons.

Bernard, P., Hardwick, K. and Javerzat, J. P. (1998). Fission yeast bub1 is a mitotic centromere protein essential for the spindle checkpoint and the preservation of correct ploidy through mitosis. *J. Cell Biol.* **143**, 1775-1787.

Bernard, P., Maure, J. F. and Javerzat, J. P. (2001). Fission yeast Bub1 is essential in setting up the meiotic pattern of chromosome segregation. *Nat. Cell. Biol.* **3**, 522-526.

Birkenbihl, R. P. and Subramani, S. (1992). Cloning and characterization of rad21 an essential gene of Schizosaccharomyces pombe involved in DNA double-strand-break repair. *Nucleic Acids Res.* **20**, 6605-6611.

Ciosk, R., Shirayama, M., Shevchenko, A., Tanaka, T., Toth, A. and Nasmyth, K. (2000). Cohesin's binding to chromosomes depends on a separate complex consisting of Scc2 and Scc4 proteins. *Mol. Cell* **5**, 243-254.

Denison, S. H., Kafer, E. and May, G. S. (1993). Mutation in the *bimD* gene of *Aspergillus nidulans* confers a conditional mitotic block and sensitivity to DNA damaging agents. *Genetics* **134**, 1085-1096.

Furuya, K., Takahashi, K. and Yanagida, M. (1998). Faithful anaphase is ensured by Mis4, a sister chromatid cohesion molecule required in S phase and not destroyed in G1 phase. *Genes Dev.* **12**, 3408-3418.

Geck, P., Szelei, J., Jimenez, J., Sonnenschein, C. and Soto, A. M. (1999). Early gene expression during androgen-induced inhibition of proliferation of prostate cancer cells: a new suppressor candidate on chromosome 13, in the BRCA2-Rb1 locus. *J. Steroid Biochem. Mol. Biol.* **68**, 41-50.

Guacci, V., Koshland, D. and Strunnikov, A. (1997). A direct link between sister chromatid cohesion and chromosome condensation revealed through the analysis of *MCD1* in *S. cerevisiae*. *Cell* **91**, 47-57.

Hartman, T., Stead, K., Koshland, D. and Guacci, V. (2000). Pds5p is an essential chromosomal protein required for both sister chromatid cohesion and condensation in Saccharomyces cerevisiae. *J. Cell Biol.* **151**, 613-626.

Hiraoka, Y., Toda, T. and Yanagida, M. (1984). The NDA3 gene of fission yeast encodes beta-tubulin: a cold-sensitive nda3 mutation reversibly blocks spindle formation and chromosome movement in mitosis. *Cell* **39**, 349-358.

Holt, C. L. and May, G. S. (1996). An extragenic suppressor of the mitosis-defective bimD6 mutation of Aspergillus nidulans codes for a chromosome scaffold protein. *Genetics* **142**, 777-787.

Huynh, A. D., Leblon, G. and Zickler, D. (1986). Indirect intergenic suppression of a radiosensitive mutant of Sordaria macrospora defective in sister-chromatid cohesiveness. *Curr. Genet.* **10**, 545-555.

Kadyk, L. C. and Hartwell, L. H. (1992). Sister chromatids are preferred over homologs as substrates for recombinational repair in *Saccharomyces cerevisiae*. *Genetics* **132**, 387-402.

Losada, A., Hirano, M. and Hirano, T. (1998). Identification of Xenopus SMC protein complexes required for sister chromatid cohesion. *Genes Dev.* **12**, 1986-1997.

Mayer, M. L., Gygi, S. P., Aebersold, R. and Hieter, P. (2001). Identification of RFC(Ctf18p, Ctf8p, Dcc1p): an alternative RFC complex required for sister chromatid cohesion in S. cerevisiae. *Mol. Cell* **7**, 959-970.

Michaelis, C., Ciosk, R. and Nasmyth, K. (1997). Cohesins: chromosomal proteins that prevent premature separation of sister chromatids. *Cell* **91**, 35-45.

Moreno, S., Klar, A. and Nurse, P. (1991). Molecular genetic analysis of fission yeast *Schizosaccharomyces pombe*. *Methods Enzymol.* **194**, 795-823.

Murakami, S., Yanagida, M. and Niwa, O. (1995). A large circular minichromosome of *Schizosaccharomyces pombe* requires a high dose of type II DNA topoisomerase for its stabilization. *Mol. Gen. Genet.* **246**, 671-679.

Neuwald, A. F. and Hirano, T. (2000). HEAT repeats associated with condensins, cohesins, and other complexes involved in chromosome-related functions. *Genome Res.* **10**, 1445-1452.

Niwa, O., Matsumoto, T. and Yanagida, M. (1986). Construction of a minichromosome by deletion and its mitotic and meiotic behaviour in fission yeast. *Mol. Gen. Genet.* **203**, 397-405.

Panizza, S., Tanaka, T., Hochwagen, A., Eisenhaber, F. and Nasmyth, K. (2000). Pds5 cooperates with cohesin in maintaining sister chromatid cohesion. *Curr Biol.* **10**, 1557-1564.

Pidoux, A. L., Uzawa, S., Perry, P. E., Cande, W. Z. and Allshire, R. C. (2000). Live analysis of lagging chromosomes during anaphase and their effect on spindle elongation rate in fission yeast. *J. Cell Sci.* **113**, 4177-4191.

Russell, P. and Nurse, P. (1986). *Schizosaccharomyces pombe* and *Saccharomyces cerevisiae*: a look at yeasts divided. *Cell* **45**, 781-782.

Sjögren, C. and Nasmyth, K. (2001). Sister chromatid cohesion is required for postreplicative double-strand break repair in *Saccharomyces cerevisiae*. *Curr. Biol.* **11**, 991-995.

Stewart, E., Chapman, C. R., Al-Khodairy, F., Carr, A. M. and Enoch, T. (1997). *rqh1*$^{+}$, a fission yeast gene related to the Bloom's and Werner's syndrome genes, is required for reversible S phase arrest. *EMBO J.* **16**, 2682-2692.

Sumara, I., Vorlaufer, E., Gieffers, C., Peters, B. H. and Peters, J. M. (2000). Characterization of vertebrate cohesin complexes and their regulation in prophase. *J. Cell Biol.* **151**, 749-762.

Tanaka, K., Yonekawa, T., Kawasaki, Y., Kai, M., Furuya, K., Iwasaki, M., Murakami, H., Yanagida, M. and Okayama, H. (2000). Fission yeast Eso1p is required for establishing sister chromatid cohesion during S phase. *Mol. Cell. Biol.* **20**, 3459-3469.

Tomonaga, T., Nagao, K., Kawasaki, Y., Furuya, K., Murakami, A., Morishita, J., Yuasa, T., Sutani, T., Kearsey, S. E., Uhlmann, F. et al. (2000). Characterization of fission yeast cohesin: essential anaphase proteolysis of Rad21 phosphorylated in the S phase. *Genes Dev.* **14**, 2757-2770.

Toth, A., Ciosk, R., Uhlmann, F., Galova, M., Schleiffer, A. and Nasmyth, K. (1999). Yeast cohesin complex requires a conserved protein, Eco1p(Ctf7), to establish cohesion between sister chromatids during DNA replication. *Genes Dev.* **13**, 320-333.

Uhlmann, F., Wernic, D., Poupart, M. A., Koonin, E. V. and Nasmyth, K. (2000). Cleavage of cohesin by the CD clan protease separin triggers anaphase in yeast. *Cell* **103**, 375-386.

van Heemst, D., James, F., Poggeler, S., Berteaux-Lecellier, V. and Zickler, D. (1999). Spo76p is a conserved chromosome morphogenesis protein that links the mitotic and meiotic programs. *Cell* **98**, 261-271.

van Heemst, D., Kafer, E., John, T., Heyting, C., van Aalderen, M. and Zickler, D. (2001). BimD/SPO76 is at the interface of cell cycle progression, chromosome morphogenesis, and recombination. *Proc. Natl Acad. Sci. USA* **98**, 6267-6272.

Wang, S. W., Toda, T., MacCallum, R., Harris, A. L. and Norbury, C. (2000a). Cid1, a fission yeast protein required for S-M checkpoint control when DNA polymerase delta or epsilon is inactivated. *Mol. Cell. Biol.* **20**, 3234-3244.

Wang, Z., Castano, I. B., De Las Penas, A., Adams, C. and Christman, M. F. (2000b). Pol kappa: a DNA polymerase required for sister chromatid cohesion. *Science* **289**, 774-779.

Wigge, P. A. and Kilmartin, J. V. (2001). The Ndc80p complex from *Saccharomyces cerevisiae* contains conserved centromere components and has a function in chromosome segregation. *J. Cell Biol.* **152**, 349-360.